



Nanoscale lamellae in an oxide dispersion strengthened steel processed by dynamic plastic deformation

Zhang, Zhenbo; Mishin, Oleg; Tao, N. R.; Pantleon, Wolfgang

Published in:
I O P Conference Series: Materials Science and Engineering

Publication date:
2014

Document Version
Publisher's PDF, also known as Version of record

[Link back to DTU Orbit](#)

Citation (APA):
Zhang, Z., Mishin, O., Tao, N. R., & Pantleon, W. (2014). Nanoscale lamellae in an oxide dispersion strengthened steel processed by dynamic plastic deformation. *I O P Conference Series: Materials Science and Engineering*, 63, 012065.

General rights

Copyright and moral rights for the publications made accessible in the public portal are retained by the authors and/or other copyright owners and it is a condition of accessing publications that users recognise and abide by the legal requirements associated with these rights.

- Users may download and print one copy of any publication from the public portal for the purpose of private study or research.
- You may not further distribute the material or use it for any profit-making activity or commercial gain
- You may freely distribute the URL identifying the publication in the public portal

If you believe that this document breaches copyright please contact us providing details, and we will remove access to the work immediately and investigate your claim.

Nanoscale lamellae in an oxide dispersion strengthened steel processed by dynamic plastic deformation

This content has been downloaded from IOPscience. Please scroll down to see the full text.

2014 IOP Conf. Ser.: Mater. Sci. Eng. 63 012065

(<http://iopscience.iop.org/1757-899X/63/1/012065>)

View [the table of contents for this issue](#), or go to the [journal homepage](#) for more

Download details:

IP Address: 192.38.67.112

This content was downloaded on 25/08/2014 at 12:31

Please note that [terms and conditions apply](#).

Nanoscale lamellae in an oxide dispersion strengthened steel processed by dynamic plastic deformation

Z B Zhang^{1,4}, O V Mishin^{1,4}, N R Tao^{2,4}, W Pantleon^{3,4}

¹ Section for Materials Science and Advanced Characterization, Department of Wind Energy, Technical University of Denmark, Risø Campus, 4000 Roskilde, Denmark

² Institute of Metal Research, Chinese Academy of Science, 110016 Shenyang, China

³ Section for Materials and Surface Engineering, Department of Mechanical Engineering, Technical University of Denmark, 2800 Kgs. Lyngby, Denmark

⁴ Sino-Danish Center for Education and Research

E-mail: zzhe@dtu.dk

Abstract. The microstructure of an oxide dispersion strengthened ferritic PM2000 steel with a strong initial $\langle 100 \rangle$ texture has been investigated after compression by dynamic plastic deformation (DPD) at room temperature to a strain of 2.1. Measurements using electron backscatter diffraction and transmission electron microscopy indicate that DPD along the $\langle 100 \rangle$ direction results in a lamellar-type microstructure, in which lamellae of the $\langle 100 \rangle$ orientation alternate with $\langle 111 \rangle$ lamellae. These lamellae have a common rotation $\langle 110 \rangle$ axis in the compression plane. The microstructure is quite heterogeneous, where regions containing very narrow lamellae (with $\langle 111 \rangle$ lamellae as narrow as 20–40 nm) and regions of comparatively broad lamellae are found.

1. Introduction

Structural refinement by plastic deformation has been extensively investigated aiming at developing high-strength materials [1,2]. In materials deformed by slip, significant structural refinement can be achieved due to grain subdivision by dislocation boundaries, for which the boundary spacing decreases with increasing strain, whereas the average misorientation angle and the fraction of high angle boundaries (HABs) increase with increasing strain [2–4]. For such materials, it has also been demonstrated that deformation at high strain rates can further accelerate the process of grain refinement [5]. For example, dynamic plastic deformation (DPD) [6] at a strain rate of $10^2 - 10^3 \text{ s}^{-1}$ has been shown to refine the microstructure in Al and Ni more effectively than deformation at comparatively low strain rates [7,8].



In the present study, structural refinement due to DPD is investigated for an oxide dispersion strengthened (ODS) ferritic steel, which is a candidate fuel cladding material for advanced nuclear reactors [9,10]. For this application, a refined microstructure may be desired to improve not only the strength, but also the irradiation tolerance [11]. To enable a detailed quantitative analysis of the deformed microstructure, both electron backscatter diffraction (EBSD) and transmission electron microscopy (TEM) are utilized in the present work.

2. Experimental

A ferritic PM2000 steel (see Table 1) with nanoscale yttria dispersoids was received in the form of a hot-extruded rod with a diameter of 13 mm [12]. This as-received material was annealed at 1200 °C for 2 hours to obtain a fully recrystallized microstructure with a coarse grain size (above 5 μm) and texture dominated by grains having a $\langle 100 \rangle$ direction aligned with the extrusion direction (ED).

Cylindrical specimens having a diameter of 6 mm and height of 9 mm were machined with their cylinder axis along the extrusion direction. Compression of the cylinders was carried out by DPD [6] at room temperature with a strain rate of $10^2 - 10^3 \text{ s}^{-1}$ by five passes to a total equivalent strain of 2.1.

Table 1 Nominal chemical composition (wt. %) of PM2000 [13].

Cr	Al	Ti	Y ₂ O ₃	Fe
20	5.5	0.5	0.5	Bal.

The microstructure of the deformed samples was investigated using both the EBSD and TEM in a section containing the compression axis (CA). TEM analysis was performed using a JEOL 2000 FX microscope. EBSD in a Zeiss Supra 35 field emission gun scanning electron microscope equipped with a Channel 5 system from HKL Technology was applied for orientation mapping with a step size of 30 nm. HABs were defined in the orientation maps as those with misorientation angles above 15°, whereas boundaries between 2° and 15° were defined as low angle boundaries (LABs).

3. Results

The deformed microstructure consists of two alternating types of lamellae closely aligned with the compression plane and having orientations with either a $\langle 100 \rangle$ direction along the CA (red in Figure 1a,b) or a $\langle 111 \rangle$ direction along the CA (blue in Figure 1a,b). The $\{110\}$ pole figure in Fig.1b reveals that the $\langle 111 \rangle$ lamellae share one 110 pole with the $\langle 100 \rangle$ lamellae. This common pole is perpendicular to the CA, i.e. the rotation axis between the $\langle 111 \rangle$ and $\langle 100 \rangle$ lamellae is in the compression plane.

Lamellae of the two different types are always separated by HABs, and contain LABs in their interior (see Figure 1a and Figure 1c). It is also apparent that the $\langle 100 \rangle$ lamellae are wider than those with the $\langle 111 \rangle$ orientation. The average width of the $\langle 100 \rangle$ and $\langle 111 \rangle$ lamellae in this microstructure is 1.4 μm and 0.5 μm , respectively. The average boundary spacing along the CA in Figure 1a is 0.3 μm . The microstructure is, however, not homogeneous, and considerable local variations are observed in the deformed sample. In some regions, original grains are subdivided by a much larger number of lamellar boundaries per area than in other regions. An example of such a well-refined region is shown in Figure 2, where very narrow lamellae are observed. Here the average boundary spacing along the CA is 0.2 μm , and the average width of the $\langle 100 \rangle$ and $\langle 111 \rangle$ lamellae in this region is 0.54 μm and 0.11 μm , respectively, which is considerably smaller than the values obtained in the region shown in Figure 1a. The width of the narrowest lamellae in Figure 2 is about 40 nm.

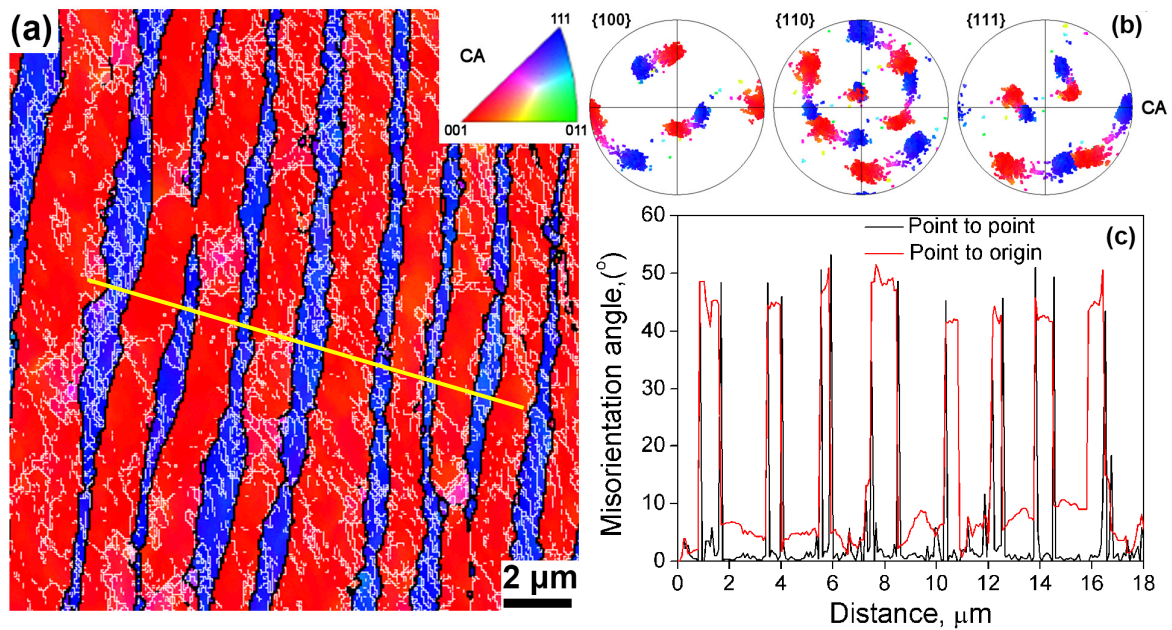


Figure 1. EBSD results for a region containing comparatively broad lamellae in PM2000 after DPD to a strain of 2.1: (a) orientation map colored according to the crystallographic direction of the CA using the color code in the inverse pole figure (see the inset). Black and white lines represent HABs and LABs, respectively; (b) {100}, {110} and {111} pole figures; (c) a misorientation profile along the yellow line in (a). The CA is horizontal.

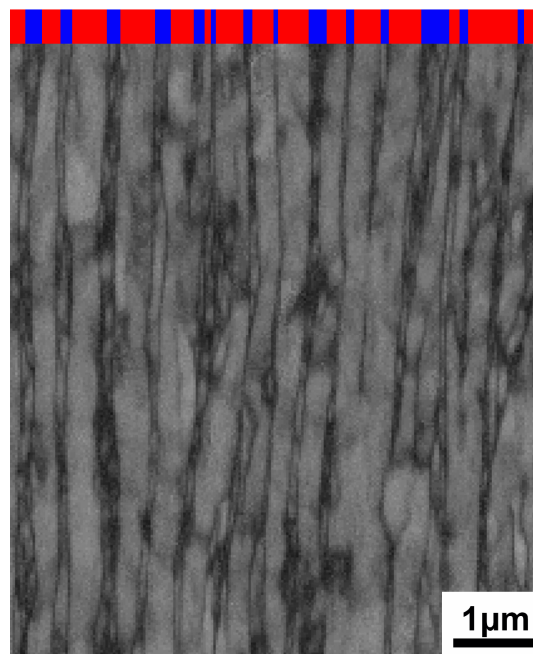


Figure 2. A band contrast map obtained by EBSD in a region with a well-refined microstructure in DPD-processed PM2000. In this map, lamellar boundaries are seen as dark lines separating light-gray lamellae. Crystallographic information is added on the top, where <100> and <111> lamellae in this region are indicated in red and blue, respectively.

TEM images (Figure 3) provide clear evidence that the width of the very narrow lamellae can vary from 20 nm to 40 nm. Similar to the EBSD data, analysis of selected area diffraction patterns and dark field images demonstrate that these very narrow bands have a $\langle 111 \rangle$ direction aligned with the CA. It is also evident that there is a large density of dislocations within the lamellae.

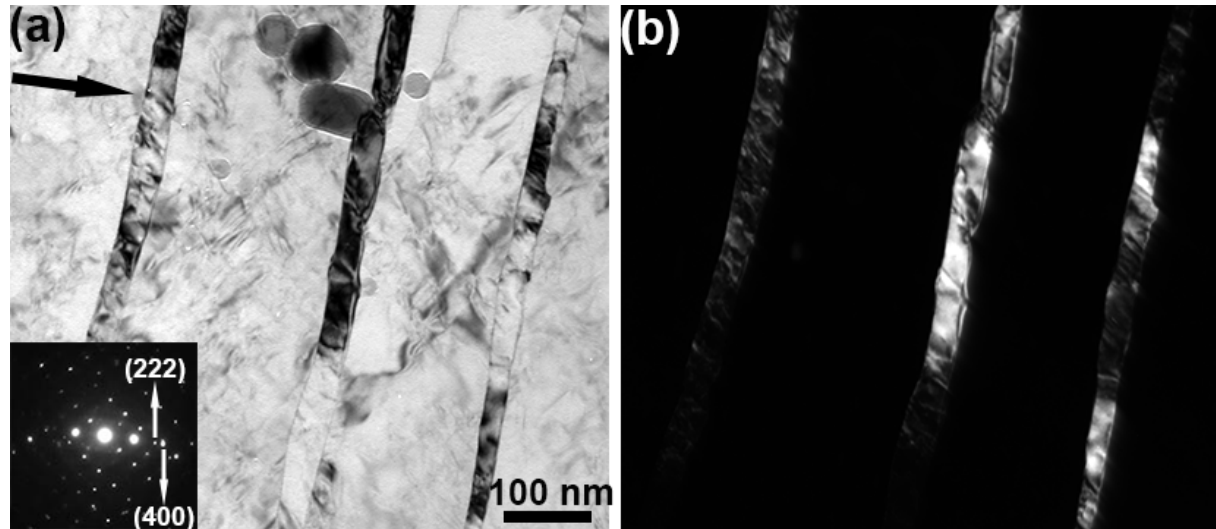


Figure 3. TEM micrographs from PM2000 after DPD to a strain of 2.1 showing comparatively wide $\langle 100 \rangle$ and very narrow $\langle 111 \rangle$ lamellae: (a) a bright field image with a selected area diffraction pattern in the inset; (b) a dark field image of the same region highlighting the $\langle 111 \rangle$ oriented lamellae. The CA is indicated by the black arrow in (a).

4. Discussion

In agreement with earlier findings reported for compressed body centered cubic materials [14,15], the texture developed in our sample is a combination of pronounced $\langle 100 \rangle$ and $\langle 111 \rangle$ components. These final texture components are spatially distributed in the form of alternating lamellae, where $\langle 100 \rangle$ lamellae are significantly wider than $\langle 111 \rangle$ lamellae. Considering that the dominant texture of the initial material was $\langle 100 \rangle$ parallel to the CA, it is suggested that the $\langle 100 \rangle$ component seen after DPD corresponds to the orientation of the matrix, in which new and narrower $\langle 111 \rangle$ lamellae are formed. In general, since the $\langle 100 \rangle$ orientation is stable, no reorientation of the lattice leading to a new $\langle 111 \rangle$ component is expected. In this respect, the observation of $\langle 111 \rangle$ lamellae in grains with the $\langle 100 \rangle$ component appears surprising. It is suggested that small regions of the original grains reoriented into $\langle 111 \rangle$ lamellae by a 55° rotation of the crystallographic lattice around a common 110 pole, as seen in the $\{110\}$ pole figure (Figure 1b). It is noteworthy that despite the existence of two crystallographically equivalent $[110]$ directions in the compression plane, all $\langle 111 \rangle$ lamellae in Figure 1a have almost identical orientations with their orientations rotated about the same $[110]$ axis (see Figure 1b). It is proposed that the occurrence of such alternating lamellae with two distinct $\langle 100 \rangle$ and $\langle 111 \rangle$ orientations and a well-defined orientation relationship between them is caused by a plastic instability similar to the bifurcation in the pattern of active slip systems during plane strain compression [16]. Such a heterogeneous activation of slip systems can be triggered by a heterogeneous character of DPD, which is consistent with our observations that the structural refinement during DPD is not uniform across the sample, where the boundary spacing varies greatly from region to region (cf. Figure 1 and Figure 2).

5. Conclusion

Compression by DPD to a strain of 2.1 is found to significantly refine the initial microstructure of the ferritic ODS steel PM2000. The deformation results in a lamellar-type microstructure, in which $\langle 100 \rangle$ lamellae alternate with $\langle 111 \rangle$ lamellae. These different lamellae have a common $[110]$ rotation axis in the compression plane. The microstructure is quite heterogeneous, where regions containing very narrow lamellae (with $\langle 111 \rangle$ lamellae as narrow as 20 – 40 nm) and regions of comparatively broad lamellae are found.

Acknowledgements

Financial support from the Sino-Danish Center for Education and Research is gratefully acknowledged. The authors are grateful to Prof. M. Heilmaier for providing the initial PM2000 sample. OVM also gratefully acknowledges the support from the Danish National Research Foundation (Grant No. DNRF86-5) and the National Natural Science Foundation of China (Grant No. 51261130091) to the Danish-Chinese Center for Nanometals.

References

- [1] Valiev R Z, Islamgaliev R K and Alexandrov I V 2000 *Prog. Mater. Sci.* **45** 103
- [2] Hansen N 2006 *Metall. Mater. Trans. A* **32** 2917
- [3] Mishin O V, Juul Jensen D and Hansen N 2010 *Metall. Mater. Trans. A* **41** 2936
- [4] Hansen N and Juul Jensen D 2011 *Mater. Sci. Technol.* **27** 1229
- [5] Gray III G T 2012 *Annu. Rev. Mater. Res.* **42** 285
- [6] Li Y S, Tao N R, and Lu K 2008 *Acta Mater.* **56** 230
- [7] Huang F, Tao N R and Lu K 2011 *J. Mater. Sci. Technol.* **27** 1
- [8] Luo Z P, Mishin O V, Zhang Y B, Zhang H W and Lu K 2012 *Scr. Mater.* **66** 335
- [9] Odette G R, Alinger M J and Wirth B D 2008 *Annu. Rev. Mater. Res.* **38** 471
- [10] Ukai S and Fujiwara M 2002 *J. Nucl. Mater.* **307** 749
- [11] Bai X M, Voter A F, Hoagland R G, Nastasi M and Uberuaga B P 2010 *Science* **327** 1631
- [12] Schneibel J H, Heilmaier M, Blum W, Hasemann G and Shanmugasundaram T 2011 *Acta Mater.* **59** 1300
- [13] Capdevila C, Chen Y L, Jones A R and Bhadeshia H K D H 2003 *ISIJ* **43** 777
- [14] Dillamore I L, Katoh H and Haslam K 1974 *Texture* **1** 151
- [15] Hu H 1974 *Texture* **1** 233
- [16] Sedlacek R, Kratochvil J, and Blum W 2001 *Phys. Stat. Sol. A* **186** 1